DOI: 10.1002/cmdc.200800113

Targeting the Open-Flap Conformation of HIV-1 Protease with Pyrrolidine-Based Inhibitors

Jark Böttcher, Andreas Blum, Stefanie Dörr, Andreas Heine, Wibke E. Diederich, and Gerhard Klebe*[a]

HIV protease is a well-established drug target in antiviral chemotherapy. Immense research efforts have been made to discover effective inhibitors, thus making the enzyme one of the most studied and best characterized proteins. Although the protease exhibits high flexibility, all approved drugs target virtually the same protein conformation. The development of viral cross-resistance demands the generation of inhibitors with novel scaffolds and deviating modes of binding. Herein we report the design and the short, high-yielding stereoselective synthesis of a series of chiral, symmetric pyrrolidine-based inhibitors targeting the open-flap conformation of the protease. The obtained co-crystal structure with one derivative provides a valuable starting point for further inhibitor design.

Introduction

Acquired immune deficiency syndrome (AIDS) is caused by infection with the human immunodeficiency virus (HIV). Despite the immense efforts in combating the epidemic, the World Health Organization (WHO) estimates that approximately 40 million people are currently infected worldwide, and thus AIDS remains one of the most serious health problems nowadays. Potent drugs targeting several stages in the viral life cycle have been developed and approved.[1] The combination of inhibitors of the viral transcriptase and protease, termed highly active antiretroviral therapy (HAART), is currently the most effective treatment for HIV-infected patients.[2,3] The introduction of HAART has increased the quality of the patient's life dramatically, however, eradication of the virus still remains an unaccomplished goal.

HIV protease is a viral aspartic proteinase that processes the viral polyprotein gene products *gag* and *gag–pol* into their functional units. The enzyme consists of 99 amino acids and is only active in dimeric form. It has been shown that inhibition of the protease leads to immature, non-infective virions, consequently making the enzyme an attractive antiretroviral drug target.[4] Unprecedented efforts in drug development have made HIV protease one of the most studied and hence best characterized enzymes; more than 240 crystal structures are assigned to its EC number (EC 3.4.23.16) in the publicly available protein data bank (PDB).[5] The first protein crystals were grown in the absence of any ligand and exhibited the space group $P4_12_12$. The corresponding structures were determined and published in 1989 (PDB IDs: 3PHV, 2HVP) and revealed an expanded active site.[6,7] The flaps covering the binding pocket exhibited a distance of more than 7 Å from the catalytically active aspartates. Because the flap region possesses extensive crystal contacts to symmetry-related molecules, the observed flap conformation was attributed to be a result of a kinetic trap during crystallization. Indeed, further structural analyses of HIV protease–inhibitor complexes unveiled that the flap region of the enzyme covers the catalytic dyad, thus leading to the active site in a closed, tunnel-shaped conformation. The first crystal structures of protein–ligand complexes (PDB IDs: 4HVP, 5HVP, and 9HVP)[8–10] hosting peptidomimetic inhibitors revealed a conserved binding mode; the ligands address the catalytic dyad via a secondary hydroxy group, and the two flaps form a parallel and an antiparallel β sheet with the ligand. Additionally, water-mediated interactions to two pivotal acceptor moieties of the ligand are formed by the NH groups of both Ile 50 being situated at the tip of the flaps. The crystal structure of HIV protease substrate complexed with an inactive Asp 25 Asn mutant showed a similar interaction pattern upon substrate binding (PDB ID: 1F7A).[11] The closed flap conformation has also been observed in the tethered dimer apo-structure in space group $P6_1$ (PDB ID: 1G6L).[12]

The open and closed flap conformations were analyzed by molecular dynamics, and for both, similar energy contents were calculated in the unbound state.[13] NMR experiments also revealed high flap flexibility, and the solution structure of the HIV protease monomer resembles the open-flap conformation.[14] Considering the multiple conformational states of the protease of nearly equal or close-by energy content, inhibitor design should be focused on addressing the protein in various states, either in the open, closed, or intermediate conformations of the flap. Particularly in the drug development of kinase inhibitors, high-affinity ligands have been developed against different states of the enzymes.[15]

[a] *J. Böttcher,[+] Dr. A. Blum,[+] S. Dörr, Dr. A. Heine, Dr. W. E. Diederich, Prof. Dr. G. Klebe*
Institut für Pharmazeutische Chemie, Philipps-Universität Marburg
Marbacher Weg 6, 35032 Marburg (Germany)
Fax: (+49) 06421-2828994
E-mail: klebe@mailer.uni-marburg.de
[+] *These authors contributed equally to this work.*

The development of HIV protease inhibitors targeting the closed conformation was extremely successful and resulted in nine FDA-approved drugs.[16] However, the clinical efficacy of these high-affinity inhibitors is strongly hampered by the increasing development of resistance. The low fidelity of the viral reverse transcriptase and the fast replication rate lead to a high mutation rate, thus providing HIV with a high degree of adaptability.[17,18] This has already resulted in resistant strains exhibiting decreased susceptibility towards all approved inhibitors, thus impeding effective antiviral therapy. Therefore, the development of new drugs preferably possessing a different mode of binding and thus circumventing the occurrence of cross-resistance is essential.

Most of the inhibitors developed so far address the catalytic dyad via a hydroxy functionality. Recently, cyclic amines have been developed as a novel anchoring group.[19,20] In a previous study, the pyrrolidine derivative **1** was designed, and the racemic mixture exhibited an affinity of 1.5 μM towards HIV-1 protease. To elucidate its binding mode, a co-crystal structure was determined and revealed the *R*,*R* enantiomer to bind with a unique interaction profile (Scheme 1). The endocyclic nitrogen

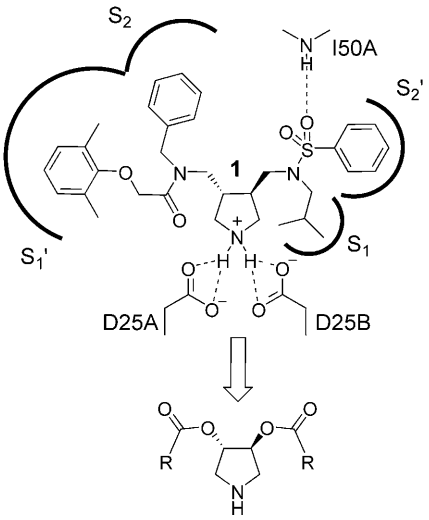

Scheme 1. Design of C_2-symmetric inhibitors starting from the co-crystal structure of **1**.

atom binds to the catalytic dyad. Poisson–Boltzmann calculations suggest the amine being protonated and both aspartates being deprotonated, resulting in strong electrostatic interactions.[21] An asymmetric flap interaction pattern is observed (Scheme 1), resulting in an unsatisfactory occupation of the sub-pockets and strong deformations of the protein structure.

Both observations might explain the only moderate affinity obtained by a ligand of such size. Based on an in-depth analysis of the crystal structure with **1**, the following hypothesis was formulated: The pyrrolidine is a suitable anchoring group, however, the interactions to the flap region and the sub-site occupancy should be improved. As an initial approach, symmetric pyrrolidine diesters with the required stereochemistry indicated in the crystal structure with **1** were designed, fulfilling the essential pharmacophore requirements. These compounds were decorated with two hydrophobic moieties to occupy the protease's sub-pockets and equipped with acceptor groups attached closer to the central pyrrolidine ring compared to **1** in order to address the flap in a geometrically more suitable way (Scheme 1).

Results and Discussion

Synthesis

3,4-Difunctionalized chiral pyrrolidines are accessible starting from tartaric acid. The synthesis of the 3*S*,4*S*-pyrrolidine diols **2** and **3** has already been described previously (Scheme 2).[22]

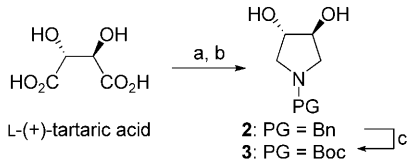

Scheme 2. Synthesis of chiral pyrrolidine-diol **3** from tartaric acid:[22] a) $BnNH_2$, xylene, reflux, 81%; b) $LiAlH_4$, THF, reflux, 65%; c) H_2, Pd/C, Boc_2O, EtOH, 90%.

Condensation of L-(+)-tartaric acid with benzylamine gave rise to the cyclic imide, which was further reduced using $LiAlH_4$ in THF at reflux. The benzyl protecting group was replaced by the Boc group via catalytic hydrogenation of **2** in the presence of Boc_2O,[23] yielding the core structure **3** (Scheme 2).

A series of diesters was prepared via condensation of **3** with the corresponding acid chlorides or the respective carboxylic acids after activation with EDC, giving rise to the enantiomerically pure diesters **4a**–**g** in high yields. The Boc group was removed by treatment with HCl in Et_2O, furnishing the inhibitors **5a**–**g** as hydrochlorides (Scheme 3). The resulting inhibitor series comprises alkyl moieties of various size (**5a**–**c**), the benzoyl derivative **5d**, and arylacetic acid derivatives (**5e**–**g**).

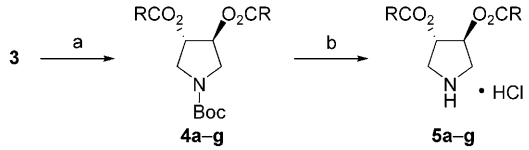

4a R = Isobutyl (81%)
4b R = Neopentyl (91%)
4c R = Cylcohexyl (77%)
4d R = Phenyl (84%)
4e R = Benzyl (66%)
4f R = CH_2-1-Naphthyl (78%)
4g R = CH_2-2-Naphthyl (74%)

5a R = Isobutyl (85%)
5b R = Neopentyl (87%)
5c R = Cylcohexyl (76%)
5d R = Phenyl (79%)
5e R = Benzyl (91%)
5f R = CH_2-1-Naphthyl (92%)
5g R = CH_2-2-Naphthyl (89%)

Scheme 3. Preparation of pyrrolidine-based inhibitors **5a**–**g**: a) RCOCl, NEt_3, CH_2Cl_2 or RCO_2H, EDC, CH_2Cl_2; b) HCl, Et_2O.

Biological data

The affinities of the pyrrolidine diesters **5a**–**g** were determined in a fluorescence-based assay towards three HIV-1 protease

variants: the wild-type originating from the BH10 isolate (PR_{WT}) and the active site point mutants Ile 50 Val (PR_{I50V}) and Ile 84 Val (PR_{I84V}). The affinities are given in Table 1.

Table 1. K_i values of the inhibitors towards the wild-type and mutant HIV proteases.[a]

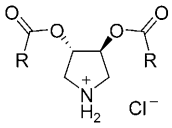

Compd	R	K_i [μM] PR_{WT}	PR_{I50V}	PR_{I84V}
5a		n.i.	n.i.	280
5b		n.i.	n.i.	43
5c		n.i.	n.i.	29
5d		n.i.	n.i.	170
5e	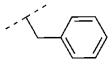	18	25	3.0
5f	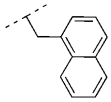	20	41	4.5
5g	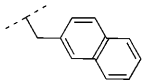	20	15	15

[a] n.i.: No inhibition observed.

In the case of PR_{WT} and PR_{I50V}, similar structure–activity relationships are observed. Whereas for the alkyl (**5a–c**) and phenyl (**5d**) substituted derivatives, no affinity could be detected, the arylacetic acid derivatives (**5e–g**) exhibit two-digit micromolar affinity. A more pronounced structure–activity relationship can be observed in the case of PR_{I84V}; for all derivatives, inhibition of PR_{I84V} was observed. The benzoyl-substituted inhibitor **5d** exhibits an affinity of 170 μM. In the case of the alkyl derivatives **5a–c**, the affinity increases with the steric demand of the substituents, ranging from 280 μM for **5a** to 29 μM for **5c**. The arylacetic acid derivatives **5e–g** show the highest affinities in the series, particularly compounds **5e** and **5f**, with K_i values of 3.0 and 4.5 μM, respectively. To elucidate the binding mode of this class of inhibitors, the most potent representatives **5e–g** were selected for co-crystallization experiments.

Structural analysis

Crystallization of HIV protease–inhibitor complexes is well established in our laboratory; peptidomimetic and pyrrolidine-type inhibitors could be crystallized in complex with the protease exhibiting binding affinities ranging from the low nanomolar to the two-digit micromolar range. Surprisingly, the crystallization of the pyrrolidine diesters **5e–g** in complex with PR_{WT} failed under the routinely applied standard crystallization conditions, however, the same conditions for PR_{I84V} were successful. In the presence of compound **5f**, large octahedral crystals were obtained, and data were collected directly after transferring the crystals to cryo-protection conditions. Remarkably, the grown crystals exhibited tetragonal symmetry in space group $P4_12_12$, typically adopted by apo-HIV protease for crystallization. In this space group, the asymmetric unit contains HIV-1 protease in its monomeric form. The functional protease dimer occupies a site coinciding with the symmetry element of a twofold axis. For clarity the amino acids of the protein chain A and its symmetry equivalent B are labeled as 1A to 99A and 1B to 99B, respectively. Due to the symmetry, all interactions within the A and the B chain are identical. For the description of contacts to other symmetry-related monomers, the chain identifiers C and D are used (Figure 1).

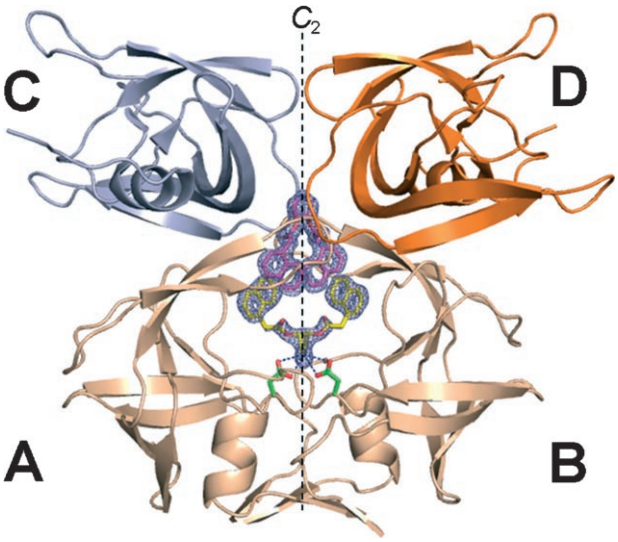

Figure 1. Crystal structure of **5f** (color-coded by atom type, α yellow, β magenta) in complex with HIV protease. The protein backbone trace is schematically illustrated in beige for monomers A and B which form the functional dimer. It is related via the indicated crystallographic C_2 axis. Within this dimer the catalytic D25A and D25B residues are displayed with green carbon atoms. Additionally, selected protein monomers from crystal packing are shown as backbone trace in blue for C and orange for D. The F_o–F_c density for the ligands is displayed at a σ level of 2.5 as blue mesh. Figures 1–4 were created using PyMol 0.99.[24]

The observed protein conformation exhibits high similarity to the apo-structures found in this space group, for example, a C_α rmsd of 0.18 Å is calculated with respect to PDB ID: 2PC0.[25] The notation of the protein sub-pockets, usually applied to HIV protease–inhibitor complexes, cannot be applied in our case, because these pockets are only regularly evolved once the flap is closed. Two molecules of **5f** are observed in the large active site cavity, comprising an area encompassed by the catalytic dyad and the flaps in the open conformation. Complex structures of HIV protease revealing a 2:1 inhibitor-to-protein ratio have been previously described, however, in contrast to the

complex of **5 f**, in these studies the second inhibitor molecule is found on the protein surface.[26,27]

Both C_2-symmetric inhibitor molecules are centered on the C_2 axis (Figure 1). However, for both molecules two different binding modes are observed, which are not related by any symmetry. Consecutively, in the following both binding modes will be described separately: the ligand situated at the catalytic dyad is referred to as **α**, whereas the ligand next to the flap region is named **β**.

Binding mode of α

As intended, **5 f** forms, with its endocyclic amino functionality, hydrogen bonds to the catalytic dyad Asp 25A (2.9 Å, 2.8 Å) and Asp 25B (Figure 2). These are the only polar interactions

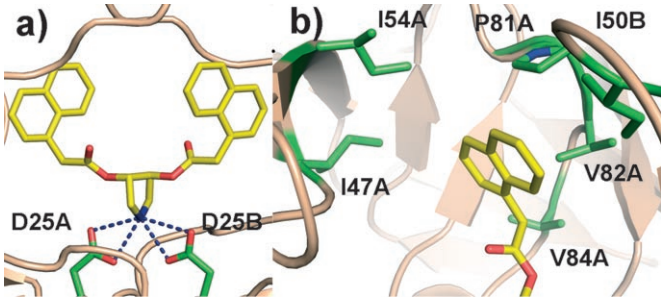

Figure 2. Binding mode of **α**, shown in yellow, color-coded by atom type; the protein backbone trace is schematically illustrated in beige. Ligand **β** is omitted for clarity. a) Polar interactions to the catalytic dyad are indicated by dashed lines; b) protein side chains in contact with the naphthyl moiety are shown in green, color-coded by atom type.

that can be observed; notably, the carbonyl ester groups thought to address the flap remain unsatisfied. The substituents at the pyrrolidine ring exhibit axial conformations. The naphthyl moieties establish numerous hydrophobic interactions to several residues of the widely opened protease binding pocket (Gly 27, Ala 28, Val 32, Ile 47, Ile 50, Ile 54, Thr 80, Pro 81, Val 82, and Val 84 of chains A and B). Neglecting the second inhibitor molecule **β** occupying part of the binding pocket, ligand **α** would have to be classified as only poorly buried (62 %). However, considering contacts to **β**, this value increases to 87 %, leading to a pronounced burial of **α**. The naphthyl moieties of **α** also form contacts to the symmetry-related molecules C and D via van der Waals contacts to the side chain of Gln 61 (Figure 4 a). However, this contact leads only to a minor increase of the burial (88 %).

Binding mode of β

The second inhibitor molecule **β** exclusively interacts with the flap region of the protease (Figure 3). Van der Waals contacts are formed to the amino acids Ile 47, Gly 48, Gly 49, Ile 50, Gly 51, Gly 52, Phe 53, and Ile 54. In contrast to **α**, the substituents at the pyrrolidine ring now exhibit equatorial conformation. The amino functionality of the pyrrolidine ring forms a

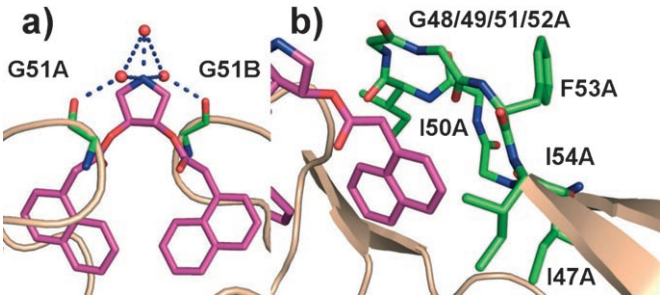

Figure 3. Binding mode of **β**, shown in magenta, color-coded by atom type, the protein backbone trace is schematically illustrated in beige. Ligand **α** is omitted for clarity. a) Polar interactions of the pyrrolidine nitrogen atom are indicated by dashed lines, waters by red spheres; b) amino acids in contact with the naphthyl moiety are shown in green, color-coded by atom type.

water-mediated hydrogen-bond network to the backbone carbonyl groups of Gly 51A and Gly 51B. Furthermore, the side chain amide functionalities of Gln 61C and Gln 61D establish hydrogen bonds to the ester carbonyl oxygen atom of the ligand (3.0 Å). The corresponding main chain carbonyls of Gln 61C and Gln 61D contribute to the above-described water-mediated hydrogen-bond interaction network involving Gly 51A and Gly 51B (Figure 4 b).

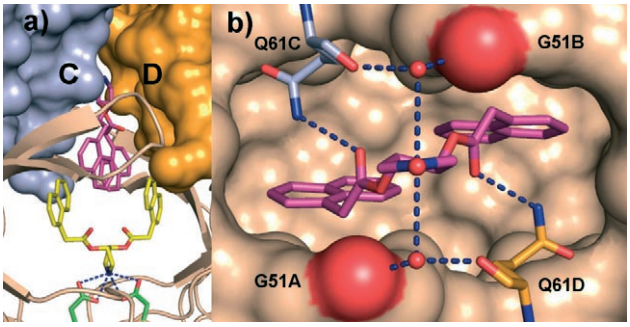

Figure 4. Interactions of **β** shown in magenta, color-coded by atom type. a) The protein backbone trace of A and B is schematically illustrated in beige, ligand **α** is shown in yellow, color-coded by atom type. Monomers C (blue) and D (orange) are shown in surface representation. b) Polar interactions are indicated by dashed lines, waters by red spheres. Monomers A and B are shown in beige surface representation except for the backbone carbonyl oxygen atom of Gly 51 in red. The interacting Gln 61 residues of chains C (blue) and D (orange) are color-coded by atom type. Ligand **α** is omitted for clarity.

Regarding only contacts formed by the inhibitor molecule **β** to the protease chains A and B, approximately half of the inhibitor's surface is buried (53 %). However, additional contacts to the second inhibitor molecule **α** increase this value to 78 %. The inhibitor molecule **β** also experiences numerous contacts to the further two symmetry-related HIV protease molecules C and D in the crystal packing. Additional van der Waals contacts are formed to amino acids Pro 39, Ile 62, Leu 63, and Ile 72 of chains C and D. Taking all contacts to interaction partners into account, ligand **β** is almost completely buried (96 %).

Discussion

The described complex, obtained by crystallization in the presence of **5 f**, is the first HIV protease co-crystal structure showing the open-flap conformation of the enzyme in which the inhibitor addresses the catalytic dyad. In the case of a previously described metallacarborane co-crystal structure of the HIV protease in an open-flap conformation, the inhibitor molecules bind to the "upper" part of the active site, and no interaction of the catalytic dyad to the inhibitor molecules was observed.[28] A crystallization strategy starting with the crystal form of the apo-protein and using soaking to prepare the complex likely prevents folding of the flap upon the accommodated ligand.[29] However, in our case the open form was obtained from a co-crystallization experiment in which the complex forms already in solution. Under such conditions any constraints from the crystal packing environment are avoided. Regarding the exceptional geometry of the co-crystal structure of **5 f**, the question arises whether it resembles the binding situation in solution. All inhibitors of our series show improved affinity against PR_{I84V} relative to the wild-type and PR_{I50V}. In the crystal structure of **5 f**, the side chain of Val 84 is in van der Waals contact to the methylene group adjacent to the ester carbonyl group of **α** (Figure 2 b). The replacement of valine 84 by isoleucine would result in decreased surface complementarities and should concomitantly lead to a decrease in affinity towards PR_{WT} which is experimentally observed. The rigid structure of the ligand core and the stereochemistry at both chiral centers presets the orientation of the introduced substituents. This hampers accommodation of the ligand at this position, thus explaining the low affinity of the even more rigid benzoyl derivative **5 d**, which lacks the flexible methylene linkers. Comparing the affinity of PR_{WT} and PR_{I50V}, no major differences are observed, which is in agreement with the only small contribution of Ile 50 to protein ligand surface contacts in case of binding **α**. According to the observed structure–activity relationship, ligands with larger substituents exhibit improved affinity. This is in good agreement with the large binding pocket, which allows for hydrophobic interactions only. Summarizing all these observations, the structure–activity relationship seems to confirm the binding mode of **α** being the biologically relevant one.

In case of **β**, neither the side chain of Val 84 nor Ile 50 is in contact with the inhibitor, thus the improved affinity towards PR_{I84V} is most likely not attributed to **β**. The naphthyl moieties establish contacts to the main chain atoms of the flap residues, the side chain of Ile 54 being the only exception, creating a comparable polar environment. Taking only chains A and B into account, no direct polar interactions are established, and the burial of the ligand remains rather incomplete. Major contribution to its burial arises from interactions with chains C and D present in the crystal packing. However, they are not present in solution, leaving an unsatisfactory binding situation for **β**. It is likely that the presence of **β** might favor crystallization of this complex by stabilizing the flap region and by interactions to neighboring protein molecules. Both ligands **α** and **β** interact extensively via π stacking of their naphthyl moieties with each other. In addition, both ligands as a bulk fill the large binding cavity. Such extensive inter-ligand interactions are only possible in the case of inhibitor **5 f**, providing a possible explanation as to why crystallization only with this particular ligand has been successful.

Summary and Conclusions

Starting from the known inhibitor **1**, a novel type of pyrrolidine-based ligand skeleton was designed. The short and high-yielding synthesis was performed via a *chiral pool* approach starting from L-(+)-tartaric acid. The resulting inhibitors **5 a**–**g** show up to low micromolar affinity against HIV protease variants. A co-crystal structure of **5 f** in complex with PR_{I84V} could be determined. Surprisingly, two inhibitor molecules **α** and **β** with mutually facing binding modes and extensive inter-ligand contacts are accommodated in the active site. In the observed binding mode **α**, the pyrrolidine nitrogen addresses the catalytic dyad as intended by our structure-guided inhibitor design. The observed structure–activity relationship can be convincingly explained considering the binding mode of **α** as the relevant one under biological conditions as well. The second inhibitor molecule **β** is only used to stabilize the flap region and presumably supports assembly and crystal growth. The open-flap conformation of HIV protease has already been postulated as a promising drug target.[30] The novel pyrrolidine-based ligands **5** are the first reported inhibitors that accommodate the protein in this conformation, at least in the crystalline state. A comparable binding mode with a closed flap would be impossible, taking the rigidity of the ligand core and the required reorganization of the protein into account. The remaining binding cavity volume would be insufficient to accommodate ligands of the size and shape of **5 a**–**g**. The co-crystal structure of **5 f** provides a valuable novel starting point for further development of HIV protease inhibitors possessing a different mode of binding compared to known drugs.

Experimental Section

Purification and crystallization of the HIV protease variants

HIV protease variants were expressed from *Escherichia coli* and purified as previously described.[31] The HIV protease–inhibitor complex was crystallized at 18 °C by the sitting-drop vapor diffusion method using a 1:1 ratio. Crystals were obtained by co-crystallization of the enzyme with an inhibitor concentration of 1 mM, final DMSO concentration of 10%. Well buffer (1 μL, 0.1 M BisTris, pH 6.5, 3.0 M NaCl) was mixed with protein solution (1 μL, 50 mM NaOAc, pH 6.5, 1 mM EDTA, 1 mM DTT) with an HIV protease concentration of 7 mg mL^{-1}. Crystals were obtained within a week and had octahedral shape. For cryo-protection the crystals were briefly soaked in mother liquor containing 25% glycerol.

Data collection, phasing, and refinement

The data set was collected using a Rigaku R-AXIS IV image plate detector using $Cu_{K\alpha}$ radiation from an in-house Rigaku RU-H3R rotating anode (Table 2). Data were processed and scaled with Denzo and Scalepack as implemented in HKL2000.[32] The structure was

Table 2. X-ray data processing and refinement for the PR_{I84V} complex of derivative **5 f**.

resolution [Å]	25–1.82
space group	$P4_12_12$
cell dimensions [Å]	a = b = 46.3, c = 101.4
highest resolution shell [Å]	1.85–1.82
no. measured reflections	101 919
no. independent reflections	10 446
completeness [%][a]	99.3 (93.7)
I/σ[a]	42.2 (10.3)
R_{sym} [%][a]	5.3 (15.9)
R_{cryst} [$F > 4\sigma F_o$; F_o]	18.7; 19.3
R_{free}[$F > 4\sigma F_o$; F_o]	24.1; 25.0
mean B-factor [Å^2] (protein)	22.5
mean B-factor [Å^2] ligand **α**	29.1
mean B-factor [Å^2] ligand **β**	21.3
mean B-factor [Å^2] water	28.2
Ramachandran plot	
most favorite geometry [%]	96.8
additionally allowed [%]	3.2
RMSD bonds [Å]	0.007
RMSD angles [°]	1.961

[a] Values in parentheses refer to the highest resolution shell.

determined by the molecular replacement method with Phaser,[33] the apo-HIV protease structure (PDB ID: 2PC0) was used as the search model. The structure refinement was continued with SHELXL-97,[34] for each refinement step at least 10 cycles of conjugate gradient minimization were performed, with restraints on bond distances, angles, and B-values. Intermittent cycles of model building were done with the program COOT.[35] The coordinates have been deposited in the PDB (http://www.rcsb.org/pdb/) with access code 3BC4.

Kinetic assay

Enzymatic assays were performed in 172 μL assay buffer (100 mM MES, 300 mM KCl, 5 mM EDTA, 1 mg mL^{-1} BSA, pH 5.5) by the addition of substrate dissolved in 4 μL DMSO, distinct inhibitor concentrations dissolved in 4 μL DMSO, and 20 μL HIV-1 protease in assay buffer to a final volume of 200 μL (final DMSO concentration 4%). The fluorogenic anthranilyl-HIV protease substrate (Abz-Thr-Ile-Nle-(*p*-NO_2-Phe)-Gln-Arg-NH_2) was purchased from Bachem. The hydrolysis of the fluorogenic substrate was recorded as the increase in fluorescence intensity (λ_{ex} = 337 nm, λ_{em} = 410 nm) over a time interval of 10 min during which the signal increased linearly.[36] The kinetic parameters of PR_{WT} (K_M = 14.6 μM), PR_{I50V} (K_M = 139 μM), and PR_{I84V} (K_M = 70 μM) were determined by the method of Lineweaver and Burk. IC_{50} values were calculated by using nonlinear regression curves for single site competitive binding analysis using the program GraFit. K_i values were calculated from the following equation: $K_i = IC_{50}[1+(S/K_M)]^{-1}$ assuming a competitive binding mechanism with a 1:1 ratio.[37] The overall error of the measurement is estimated to be ±40%.

General

Reported yields refer to the analytically pure product obtained by column chromatography or recrystallization. All proton and carbon NMR spectra were recorded on a Jeol Eclipse+ Spectrometer (^{1}H NMR: 500 MHz, ^{13}C NMR: 125 MHz) using TMS as internal standard (0.0 ppm). ^{13}C NMR spectra were referenced to $CDCl_3$ (77.16 ppm). The values of chemical shifts (δ) are given in ppm, and coupling constants (J) are given in Hz. Abbreviations: br = broad, s = singlet, d = doublet, t = triplet, q = quartet, smul = symmetric multiplet, m = multiplet. Mass spectra were obtained from a double focusing sector field Micromass VG-Autospec spectrometer. Combustion analyses were determined on a Vario Micro Cube by Elementar Analysen GmbH, and the results indicated by symbols for the elements were within ±0.4% of theoretical values. Melting points were determined using a Leitz HM-Lux apparatus and are uncorrected. Flash chromatography was performed using a Büchi Sepacore Flash MPLC system and silica gel 60 (0.04–0.063 mm) purchased from Macherey–Nagel, and solvents as indicated. TLC was carried out using 0.2 mm aluminum plates coated with silica gel 60 F_{254} by Merck and visualized by UV detection. Solvents and reagents that are commercially available were used without further purification unless otherwise noted. All moisture-sensitive reactions were carried out using oven-dried glassware under a positive stream of argon. Compound **2** was prepared according to a reported procedure.[22]

(3*S*,4*S*)-1-Boc-3,4-Dihydroxypyrrolidine (3): (3*S*,4*S*)-1*N*-benzyl-3,4-dihydroxypyrrolidine (**2**) (2.00 g, 10.5 mmol) was dissolved in EtOH (70 mL) followed by the addition of Boc_2O (2.51 g, 11.5 mmol) and Pd/C (334 mg). After stirring the reaction mixture under H_2 atmosphere for 16 h, the catalyst was removed by filtration through a pad of Celite, and the filtrate was concentrated. The residual yellow oil was recrystallized from 20 mL EtOAc. The crystals were collected by filtration, washed with cold EtOAc, and dried yielding 1.91 g (90%) of **3**. The compound exhibited similar physical and spectroscopic data as described earlier.[38] Beige needles; mp: 161 °C; ^{1}H NMR (500 MHz, $CDCl_3$): δ = 1.49 (s, 9H), 3.28 (dbr, J = 10.1, 1H), 3.34 (dbr, J = 8.9, 1H), 3.61 (dbr, J = 8.5, 2H), 4.06–4.11 (m, 2H), 4.71 ppm (sbr, 2H).

General procedure A for the preparation of diesters using acid chlorides: Pyrrolidine diol **3** (305 mg, 1.5 mmol) was dissolved in CH_2Cl_2 (5 mL) followed by the addition of acid chloride (4.5 mmol), dropwise addition of triethylamine (630 μL, 4.5 mmol), and a catalytic amount of 4-dimethylaminopyridine (DMAP). After stirring the reaction mixture for 13 h, a solution of $NaHCO_3$ (5 mL, sat.) was added, and the mixture was stirred for 15 min. The aqueous phase was separated and extracted with CH_2Cl_2 (5 × 5 mL). The combined organic phases were washed with brine (3 × 10 mL), dried over $MgSO_4$, filtered, and evaporated. The residue was further purified by MPLC.

General procedure B for the preparation of diesters by coupling of carboxylic acids with EDC: Pyrrolidine diol **3** (305 mg, 1.5 mmol), acid (3.15 mmol), and a catalytic amount of DMAP were dissolved in CH_2Cl_2 (10 mL), and the solution was cooled to 0 °C. After addition of 3-(3-dimethylaminopropyl)-1-ethylcarbodiimide hydrochloride (EDC) (604 mg, 3.15 mmol) the mixture was stirred for 1 h, allowed to warm to room temperature, and stirred overnight. The solvent was evaporated, and the residue was taken up with 10 mL H_2O and 20 mL EtOAc. The aqueous phase was separated and extracted with EtOAc (3 × 15 mL). The combined organic phases were washed with brine (3 × 10 mL), dried over $MgSO_4$, filtered, and evaporated. The residue was further purified by MPLC.

General procedure C for Boc deprotection: The pyrrolidine diester (0.75 mmol) was dissolved in 2 M HCl in Et_2O (5 mL) and stirred at room temperature until TLC indicated complete conversion. The solution was decanted from the precipitated hydrochlo-

ride, which was washed thoroughly with dry ether and further purified by MPLC.

(3*S*,4*S*)-1-Boc-3,4-Bis-(3-methylbutyryloxy)pyrrolidine (4a): Following the general procedure B, use of 3-methylbutyric acid (348 μL, 3.15 mmol) and purification by FC (hexane/MTBE 3:1) yielded **4a** (490 mg, 81%). Colorless crystals; mp: 176 °C; ^{1}H NMR (500 MHz, $CDCl_3$): δ = 0.95 (s, 12H), 1.46 (s, 9H), 2.08 (smul, 2H), 2.20 (d, J = 7.3, 4H), 3.43 (d, J = 13.1, 1H), 3.52 (d, J = 13.1, 1H), 3.66 (dd, J = 13.1, J = 4.4, 1H), 3.69 (dd, J = 12.6, J = 4.4, 1H), 5.11 (d, J = 3.0, 1H), 5.15 ppm (d, J = 3.2, 1H); ^{13}C NMR (125 MHz, $CDCl_3$): δ = 22.4, 25.8, 28.5, 43.3, 49.9, 50.4, 74.1, 75.1, 80.1, 154.3, 170.3, 170.5 ppm; MS (ESI) m/z = 394 (22, $[M+Na]^+$), 765 (100, $[2M+Na]^+$), 1136 (11, $[3M+Na]^+$; Anal. ($C_{19}H_{33}NO_6$) C, H, N.

(3*S*,4*S*)-1-Boc-3,4-Bis-(3,3-dimethylbutyryloxy)pyrrolidine (4b): According to general procedure A, use of 3,3-dimethylbutyric acid chloride (625 μL, 4.50 mmol) and purification by FC (hexane/MTBE 6:1) gave rise to **4b** (545 mg, 91%). Colorless crystals; mp: 49 °C; ^{1}H NMR (500 MHz, $CDCl_3$): δ = 1.02 (s, 18H), 1.46 (s, 9H), 2.21 (s, 4H), 3.45 (d, J = 12.6, 1H), 3.53 (d, J = 12.6, 1H), 3.65 (dd, J = 13.0, J = 4.4, 1H), 3.69 (dd, J = 13.1, J = 4.6, 1H), 5.10 (d, J = 3.7, 1H), 5.15 ppm (d, J = 3.7, 1H); ^{13}C NMR (125 MHz, $CDCl_3$): δ = 25.8, 28.4, 29.7, 31.0, 47.9, 50.0, 50.5, 74.1, 75.0, 80.1, 154.3, 171.1, 171.2 ppm; MS (ESI) m/z = 422 (33, $[M+Na]^+$), 821 (100, $[2M+Na]^+$), 1220 (9, $[3M+Na]^+$); Anal. ($C_{21}H_{37}NO_6$) C, H, N.

(3*S*,4*S*)-1-Boc-3,4-Bis-cyclohexanylcarbonyloxypyrrolidine (4c): Following general procedure A, use of cyclohexyl carboxylic acid chloride (611 μL, 4.50 mmol) and purification by FC (hexane/MTBE 5:1) furnished **4c** (489 mg, 77%). Colorless crystals; mp: 92 °C; ^{1}H NMR (500 MHz, $CDCl_3$): δ = 1.17–1.33 (m, 6H), 1.37–1.46 (m, 4H), 1.47 (s, 9H), 1.61–1.67 (m, 2H), 1.70–1.78 (m, 4H), 1.83–1.92 (m, 4H), 2.30 (smul, 2H), 3.40 (d, J = 12.6, 1H), 3.49 (d, J = 12.8, 1H), 3.66 (smul, 2H), 5.09 (dbr, J = 3.4, 1H), 5.13 ppm (dbr, J = 3.2, 1H); ^{13}C NMR (125 MHz, $CDCl_3$): δ = 25.4, 25.7, 28.6, 28.9, 29.0, 43.0, 49.9, 50.4, 74.0, 74.9, 80.1, 154.5, 174.8, 175.0 ppm; MS (ESI) m/z = 446 (52, $[M+Na]^+$), 869 (100, $[2M+Na]^+$), 1292 (11, $[3M+Na]^+$); Anal. ($C_{23}H_{37}NO_6$) C, H, N.

(3*S*,4*S*)-1-Boc-3,4-Bis-benzoyloxypyrrolidine (4d): According to general procedure A, use of benzoyl chloride (522 μL, 4.50 mmol) and purification by FC (hexane/MTBE 5:1) yielded **4d** (518 mg, 84%). Colorless crystals; mp: 158 °C; ^{1}H NMR (500 MHz, $CDCl_3$): δ = 1.41 (s, 9H), 3.59 (d, J = 12.6, 2H), 3.84–3.91 (m, 2H), 5.52 (sbr, 2H), 7.56 (t, J = 7.8, 4H), 7.70 (t, J = 7.5, 2H), 8.01 ppm (d, J = 7.3, 4H); ^{13}C NMR (125 MHz, $CDCl_3$): δ = 28.6, 50.0, 50.6, 75.0, 75.9, 80.3, 128.6, 129.3, 129.4, 129.9, 133.6, 133.7, 154.6, 165.4, 165.5 ppm; MS (ESI) m/z = 434 (98, $[M+Na]^+$), 845 (100, $[2M+Na]^+$); Anal. ($C_{23}H_{25}NO_6$) C, H, N.

(3*S*,4*S*)-1-Boc-3,4-Bis-phenylacetoxypyrrolidine (4e): Following general procedure A, use of phenylacetyl chloride (569 μL, 4.50 mmol) and purification by FC (hexane/MTBE 4:1) gave rise to **4e** (435 mg, 66%). Yellow oil; ^{1}H NMR (500 MHz, $CDCl_3$): δ = 1.46 (s, 9H), 3.37 (d, J = 13.1, 1H), 3.50 (d, J = 15.4, 1H), 3.55–3.79 (m, 6H), 5.09 (d, J = 2.3, 1H), 5.13 (d, J = 2.8, 1H), 7.13–7.39 ppm (m, 10H); ^{13}C NMR (125 MHz, $CDCl_3$): δ = 28.5, 40.2, 49.7, 50.2, 74.6, 75.5, 80.1, 127.5, 128.8, 129.2, 133.3, 154.3, 170.3, 170.5 ppm; MS (ESI) m/z = 462 (100, $[M+Na]^+$), 901 (96, $[2M+Na]^+$); Anal. ($C_{25}H_{29}NO_6$) C, H, N; C: calcd: 68.32, found: 69.21.

(3*S*,4*S*)-1-Boc-3,4-Bis-(1-naphthalen-1-ylacetoxy)pyrrolidine (4f): According to general procedure B, use of 1-naphthylacetic acid (587 mg, 3.15 mmol) and purification by FC (hexane/MTBE 3:1) furnished **4f** (631 mg, 78%). Colorless crystals; mp: 86 °C; ^{1}H NMR (500 MHz, $CDCl_3$): δ = 1.41 (s, 9H), 3.25 (d, J = 12.6, 1H), 3.38 (dd, J = 12.7, J = 4.5, 1H), 3.43 (d, J = 13.0, 1H), 3.49 (dd, J = 12.7, J = 4.2, 1H), 4.03 (sbr, 4H), 5.01 (d, J = 3.7, 1H), 5.07 (d, J = 3.4, 1H), 7.38 (d, J = 6.9, 2H), 7.39 (dd, J = 8.0, J = 7.1, 2H), 7.44–7.52 (m, 4H), 7.77 (d, J = 8.0, 2H), 7.84 (d, J = 8.3, 2H), 7.87 ppm (d, J = 8.0, 2H); ^{13}C NMR (125 MHz, $CDCl_3$): δ = 28.5, 39.0, 49.6, 50.0, 74.6, 75.5, 80.0, 123.6, 125.5, 126.0, 126.6, 128.1, 128.4, 128.9, 129.8, 132.0, 133.9, 154.2, 170.2, 170.4 ppm; MS (ESI) m/z = 1101 (100, $[2M+Na]^+$); Anal. ($C_{33}H_{33}NO_6 \cdot 2.5\,H_2O$) C, H, N.

(3*S*,4*S*)-1-Boc-3,4-Bis-(2-naphthalen-1-ylacetoxy)pyrrolidine (4g): Following general procedure B, use of 2-naphthylacetic acid (587 mg, 3.15 mmol) and purification by FC (hexane/MTBE 3:1) gave rise to **4g** (599 mg, 74%). Colorless crystals; mp: 137 °C; ^{1}H NMR (500 MHz, $CDCl_3$): δ = 1.42 (s, 9H), 3.38 (d, J = 12.6, 1H), 3.54 (d, J = 12.8, 1H), 3.66 (dd, J = 12.7, J = 4.7, 1H), 3.68 (dd, J = 12.6, J = 4.6, 1H), 3.78 (sbr, 4H), 5.14 (d, J = 2.8, 1H), 5.18 (d, J = 3.2, 1H), 7.36 (d, J = 8.3, 2H), 7.43–7.50 (m, 4H), 7.70 (sbr, 2H), 7.77–7.84 ppm (m, 6H); ^{13}C NMR (125 MHz, $CDCl_3$): δ = 28.5, 41.4, 49.7, 50.2, 74.4, 75.6, 80.2, 126.1, 126.4, 127.2, 127.7, 127.8, 128.1, 128.5, 130.8, 132.7, 133.5, 154.4, 170.4, 170.5 ppm; MS (ESI) m/z = 562 (100, $[M+Na]^+$); Anal. ($C_{33}H_{33}NO_6 \cdot 0.5\,H_2O$) C, H, N.

(3*S*,4*S*)-3,4-Bis-(3-methylbutyryloxy)pyrrolidine hydrochloride (5a): Following general procedure C, use of **4a** (231 mg, 0.62 mmol) and purification by FC (CH_2Cl_2/MeOH 95:5) yielded **5a** (196 mg, 85%). Colorless hygroscopic crystals; ^{1}H NMR (500 MHz, $CDCl_3$): δ = 0.95 (sbr, 12H), 2.09 (sbr, 2H), 2.26 (sbr, 4H), 3.32–3.81 (m, 4H), 5.25 (sbr, 2H), 10.40 ppm (sbr, 2H); ^{13}C NMR (125 MHz, $CDCl_3$): δ = 22.4, 25.5, 42.9, 49.6, 74.1, 171.5 ppm; MS (ESI) m/z = 272 (100, $[M+H]^+$), 543 (4, $[2M+H]^+$); Anal. ($C_{14}H_{25}NO_4 \cdot HCl$) C, H, N, Cl.

(3*S*,4*S*)-3,4-Bis-(3,3-dimethylbutyryloxy)pyrrolidine hydrochloride (5b): According to general procedure C, use of **4b** (300 mg, 0.75 mmol) and purification by FC (CH_2Cl_2/MeOH 95:5) gave rise to **5b** (219 mg, 87%). Colorless crystals; mp: 176 °C; ^{1}H NMR (500 MHz, $CDCl_3$): δ = 1.03 (s, 18H), 2.27 (s, 4H), 3.39 (d, J = 13.1, 2H), 3.59 (dd, J = 13.2, J = 4.0, 2H), 5.22 ppm (d, J = 3.9, 2H); ^{13}C NMR (125 MHz, $CDCl_3$): δ = 29.6, 30.9, 47.4, 49.5, 74.6, 170.8 ppm; MS (ESI) m/z = 300 (100, $[M+H]^+$), 599 (27, $[2M+Na]^+$); Anal. ($C_{16}H_{29}NO_4 \cdot HCl$) C, H, N, Cl; C: calcd: 57.22, found: 58.50.

(3*S*,4*S*)-3,4-Bis-cyclohexanecarbonyloxypyrrolidine hydrochloride (5c): Following general procedure C, use of **4c** (318 mg, 0.75 mmol) and purification by FC (CH_2Cl_2/MeOH 95:5) furnished **5c** (204 mg, 76%). Colorless crystals; mp: 186 °C; ^{1}H NMR (500 MHz, $CDCl_3$): δ = 1.17–1.33 (m, 6H), 1.38–1.49 (m, 4H), 1.60–1.64 (m, 2H), 1.71–1.79 (m, 4H), 1.92 (t, J = 15.0, 4H), 2.37 (tt, J = 11.2, J = 3.5, 2H), 3.49 (dbr, J = 11.9, 2H), 3.59–3.69 (smul, 2H), 5.24 (d, J = 3.2, 2H), 10.54 ppm (sbr, 2H); ^{13}C NMR (125 MHz, $CDCl_3$): δ = 25.2, 25.3, 25.6, 28.7, 28.9, 42.7, 48.9, 74.0, 174.5 ppm; MS (ESI) m/z = 324 (100, $[M+H]^+$); Anal. ($C_{18}H_{29}NO_4 \cdot HCl$) C, H, N, Cl.

(3*S*,4*S*)-3,4-Bis-benzoyloxypyrrolidine hydrochloride (5d): According to general procedure C, use of **4d** (309 mg, 0.75 mmol) and purification by FC (CH_2Cl_2/MeOH 95:5) yielded **5d** (206 mg, 79%). Colorless crystals; mp: 182 °C; ^{1}H NMR (500 MHz, $CDCl_3$): δ = 3.58–4.09 (m, 4H), 5.70 (sbr, 2H), 7.45 (sbr, 4H), 7.59 (sbr, 2H), 8.31 ppm (s, 4H); ^{13}C NMR (125 MHz, $CDCl_3$): δ = 50.0, 74.9, 128.4, 130.5, 134.0, 164.9 ppm; MS (ESI) m/z = 312 (100, $[M+H]^+$); Anal. ($C_{18}H_{17}NO_4 \cdot HCl$) C, H, N, Cl.

(3*S*,4*S*)-3,4-Bis-phenylacetoxypyrrolidine hydrochloride (5e): Following general procedure C, use of **4e** (330 mg, 0.75 mmol) and purification by FC (CH_2Cl_2/MeOH 95:5) gave rise to **5e** (407 mg,

91%). Orange oil; ^{1}H NMR (500 MHz, $CDCl_3$): δ = 3.51–3.76 (m, 8H), 5.20 (s, 2H), 7.14–7.41 (m, 10H), 10.45 ppm (sbr, 2H); ^{13}C NMR (125 MHz, $CDCl_3$): δ = 40.8, 48.9, 74.6, 127.5, 128.7, 129.4, 132.8, 170.2 ppm; MS (ESI) m/z = 340 (100, $[M+H]^+$), 679 (14, $[2M+H]^+$); Anal. ($C_{20}H_{21}NO_4 \cdot HCl \cdot 0.5\,H_2O$) C, H, N, Cl.

(3*S*,4*S*)-3,4-Bis-(1-naphthalen-1-ylacetoxy)pyrrolidine hydrochloride (5f): According to general procedure C, use of **4f** (378 mg, 0.70 mmol) and purification by FC (CH_2Cl_2/MeOH 95:5) furnished **5f** (303 mg, 92%). Colorless hygroscopic crystals; ^{1}H NMR (500 MHz, $CDCl_3$): δ = 3.59 (sbr, 4H), 4.14–4.23 (smul, 4H), 5.17 (sbr, 2H), 7.41–7.48 (m, 4H), 7.50 (t, J = 8.0, 2H), 7.59 (t, J = 7.3, 2H), 7.81 (d, J = 7.1, 2H), 7.87 (d, J = 8.0, 2H), 7.99 (d, J = 8.3, 2H), 10.62 ppm (sbr, 1H); ^{13}C NMR (125 MHz, $CDCl_3$): δ = 38.5, 49.1, 74.6, 123.8, 125.6, 126.0, 126.8, 128.4, 128.6, 128.9, 129.3, 132.0, 133.9, 170.1 ppm; MS (ESI) m/z = 440 (100, $[M+H]^+$), 879 (12, $[2M+H]^+$); Anal. ($C_{28}H_{25}NO_4 \cdot 0.5\,H_2O \cdot HCl$) C, H, N, Cl; C: calcd: 69.34, found: 68.74.

(3*S*,4*S*)-3,4-Bis-(2-naphthalen-1-ylacetoxy)pyrrolidine hydrochloride (5g): Following general procedure C, use of **4g** (404 mg, 0.75 mmol) and purification by FC (CH_2Cl_2/MeOH 95:5) gave rise to **5g** (315 mg, 89%). Orange crystals; mp: 147 °C; ^{1}H NMR (500 MHz, $CDCl_3$): δ = 3.56 (s, 1H), 3.58 (s, 1H), 3.62 (d, J = 3.7, 1H), 3.64 (d, J = 3.4, 1H), 3.82–3.92 (smul, 4H), 5.23 (d, J = 3.4, 2H), 7.41 (dd, J = 8.4, J = 1.7, 2H), 7.43–7.47 (m, 4H), 7.73 (sbr, 2H), 7.77–7.82 ppm (m, 6H); ^{13}C NMR (125 MHz, $CDCl_3$): δ = 41.0, 49.0, 74.7, 126.1, 126.3, 127.3, 127.7, 127.8, 128.4, 128.5, 130.3, 132.7, 133.5, 170.2 ppm; MS (ESI) m/z = 440 (100, $[M+H]^+$), 879 (12, $[2M+H]^+$); Anal. ($C_{28}H_{25}NO_4 \cdot 0.5\,H_2O \cdot HCl$) C, H, N, Cl.

Acknowledgements

This work was supported by a fellowship (A.B.) from the Fonds der Chemischen Industrie (FCI).

Keywords: drug design · HIV protease · inhibitors · open-flap conformation · pyrrolidines

[1] R. J. Pomerantz, D. L. Horn, *Nat. Med.* **2003**, *9*, 867–873.
[2] J. A. Bartlett, R. DeMasi, J. Quinn, C. Moxham, F. Rousseau, *AIDS* **2001**, *15*, 1369–1377.
[3] R. M. Gulick, J. W. Mellors, D. Havlir, J. J. Eron, A. Meibohm, J. H. Condra, F. T. Valentine, D. McMahon, C. Gonzalez, L. Jonas, E. A. Emini, J. A. Chodakewitz, R. Isaacs, D. D. Richman, *Ann. Intern. Med.* **2000**, *133*, 35–39.
[4] N. E. Kohl, E. A. Emini, W. A. Schleif, L. J. Davis, J. C. Heimbach, R. A. F. Dixon, E. M. Scolnick, I. S. Sigal, *Proc. Natl. Acad. Sci. USA* **1988**, *85*, 4686–4690.
[5] F. C. Bernstein, T. F. Koetzle, G. J. B. Williams, E. F. Meyer, Jr., M. D. Brice, J. R. Rodgers, O. Kennard, T. Shimanouchi, M. Tasumi, *J. Mol. Biol.* **1977**, *112*, 535–542.
[6] R. Lapatto, T. Blundell, A. Hemmings, J. Overington, A. Wilderspin, S. Wood, J. R. Merson, P. J. Whittle, D. E. Danley, K. F. Geoghegan, S. J. Hawrylik, S. E. Lee, K. G. Scheld, P. M. Hobart, *Nature* **1989**, *342*, 299–302.
[7] M. A. Navia, P. M. D. Fitzgerald, B. M. McKeever, C.-T. Leu, J. C. Heimbach, W. K. Herber, I. S. Sigal, P. L. Darke, J. P. Springer, *Nature* **1989**, *337*, 615–620.
[8] M. Miller, J. Schneider, B. K. Sathyanarayana, M. V. Toth, G. R. Marshall, L. Clawson, L. Selk, S. B. Kent, A. Wlodawer, *Science* **1989**, *246*, 1149–1152.
[9] P. M. D. Fitzgerald, B. M. McKeever, J. F. VanMiddlesworth, J. P. Springer, J. C. Heimbach, C.-T. Leu, W. K. Herber, R. A. F. Dixon, P. L. Darke, *J. Biol. Chem.* **1990**, *265*, 14209–14219.
[10] J. Erickson, D. J. Neidhart, J. VanDrie, D. J. Kempf, X. C. Wang, D. W. Norbeck, J. J. Plattner, J. W. Rittenhouse, M. Turon, N. N. Wideburg, W. E. Kohlbrenner, R. Simmer, R. Helfrich, D. A. Paul, M. Knigge, *Science* **1990**, *249*, 527–533.
[11] M. Prabu-Jeyabalan, E. Nalivaika, C. A. Schiffer, *J. Mol. Biol.* **2000**, *301*, 1207–1220.
[12] B. Pillai, K. K. Kannan, M. V. Hosur, *Proteins Struc. Funct. Genet.* **2001**, *43*, 57–64.
[13] S. W. Rick, J. W. Erickson, S. K. Burt, *Proteins Struc. Funct. Genet.* **1998**, *32*, 7–16.
[14] R. Ishima, D. A. Torchia, S. M. Lynch, A. M. Gronenborn, J. M. Louis, *J. Biol. Chem.* **2003**, *278*, 43311–43319.
[15] Y. Liu, N. S. Gray, *Nat. Chem. Biol.* **2006**, *2*, 358–364.
[16] A. Wlodawer, J. W. Erickson, *Annu. Rev. Biochem.* **1993**, *62*, 543–585.
[17] H. Ohtaka, S. Muzammil, A. Schön, A. Velazquez-Campoy, S. Vega, E. Freire, *Int. J. Biochem. Cell Biol.* **2004**, *36*, 1787–1799.
[18] R. T. D'Aquila, J. M. Schapiro, F. Brun-Vézinet, B. Clotet, B. Conway, L. M. Demeter, R. M. Grant, V. A. Johnson, D. R. Kuritzkes, C. Loveday, R. W. Shafer, D. D. Richman, *Topics in HIV Medicine* **2002**, *10*, 21–25.
[19] E. Specker, J. Böttcher, H. Lilie, A. Heine, A. Schoop, G. Müller, N. Griebenow, G. Klebe, *Angew. Chem.* **2005**, *117*, 3200–3204; *Angew. Chem. Int. Ed.* **2005**, *44*, 3140–3144.
[20] E. Specker, J. Böttcher, S. Brass, A. Heine, H. Lilie, A. Schoop, G. Müller, N. Griebenow, G. Klebe, *ChemMedChem* **2006**, *1*, 106–117.
[21] P. Czodrowski, C. A. Sotriffer, G. Klebe, *J. Chem. Inf. Model.* **2007**, *47*, 1590–1598.
[22] A. M. d'A. Rocha Gonsalves, M. E. S. Serra, D. Murtinho, V. F. Silva, A. Matos Beja, J. A. Paixão, M. Ramos Silva, L. Alte da Veiga, *J. Mol. Catal. A* **2003**, *195*, 1–9.
[23] R. M. Rodríguez Sarmiento, B. Wirz, H. Iding, *Tetrahedron: Asymmetry* **2003**, *14*, 1547–1551.
[24] W. L. DeLano, DeLano Scientific, San Carlos, CA, (USA) **2002**.
[25] H. Heaslet, R. Rosenfeld, M. Giffin, Y.-C. Lin, K. Tam, B. E. Torbett, J. H. Elder, D. E. McRee, C. D. Stout, *Acta Crystallogr. Sect. D* **2007**, *63*, 866–875.
[26] J. Brynda, P. Řezáčová, M. Fábry, M. Hořejší, R. Štouračová, M. Souček, M. Hradílek, J. Konvalinka, J. Sedláček, *Acta Crystallogr. Sect. D* **2004**, *60*, 1943–1948.
[27] A. Y. Kovalevsky, F. Liu, S. Leshchenko, A. K. Ghosh, J. M. Louis, R. W. Harrison, I. T. Weber, *J. Mol. Biol.* **2006**, *363*, 161–173.
[28] P. Cígler, M. Kozísek, P. Řezáčová, J. Brynda, Z. Otwinowski, J. Pokorná, J. Plesek, B. Grüner, L. Dolecková-Maresová, M. Másа, J. Sedláček, J. Bodem, H.-G. Kräusslich, V. Král, J. Konvalinka, *Proc. Natl. Acad. Sci. USA* **2005**, *102*, 15394–15399.
[29] B. C. Logsdon, J. F. Vickrey, P. Martin, G. Proteasa, J. I. Koepke, S. R. Terlecky, Z. Wawrzak, M. A. Winters, T. C. Merigan, L. C. Kovari, *J. Virol.* **2004**, *78*, 3123–3132.
[30] P. Martin, J. F. Vickrey, G. Proteasa, Y. L. Jimenez, Z. Wawrzak, M. A. Winters, T. C. Merigan, L. C. Kovari, *Structure* **2005**, *13*, 1887–1895.
[31] A. Taylor, D. P. Brown, S. Kadam, M. Maus, W. E. Kohlbrenner, D. Weigl, M. C. Turon, L. Katz, *Appl. Microbiol. Biotechnol.* **1992**, *37*, 205–210.
[32] Z. Otwinowski, W. Minor in *Methods Enzymol., Vol. 276* (Ed.: C. W. Carter, Jr.), Academic Press, **1997**, pp. 307–326.
[33] L. C. Storoni, A. J. McCoy, R. J. Read, *Acta Crystallogr. Sect. D* **2004**, *60*, 432–438.
[34] G. M. Sheldrick, T. R. Schneider in *Methods Enzymol., Vol. 277* (Eds.: W. C. J. Charles, M. S. Robert), Academic Press, **1997**, pp. 319–343.
[35] P. Emsley, K. Cowtan, *Acta Crystallogr. Sect. D* **2004**, *60*, 2126–2132.
[36] M. V. Toth, G. R. Marshall, *Int. J. Pept. Protein Res.* **1990**, *36*, 544–550.
[37] C. Yung-Chi, W. H. Prusoff, *Biochem. Pharmacol.* **1973**, *22*, 3099–3108.
[38] R. Siedlecka, E. Wojaczynska, J. Skarzewski, *Tetrahedron: Asymmetry* **2004**, *15*, 1437–1444.

Received: April 11, 2008
Revised: July 22, 2008
Published online on August 21, 2008

